17th World Conference on Earthquake Engineering, 17WCEE

Sendai, Japan - September 13th to 18th 2020

A SIMPLIFIED METHOD FOR THE SEISMIC ANALYSIS OF CUT-AND-COVER STRUCTURES. TOWARDS THE UNIFICATION OF CRITERIA

C. Gordo-Monsó[(1)], J. González-Galindo[(2)], C. Olalla-Marañón[(3)]

[(1)] *Adjunct Professor, Universidad Politécnica de Madrid, carlos.gordom@upm.es*
[(2)] *Assistant Professor, Universidad Politécnica de Madrid, jesus.gonzalezg@upm.es*
[(3)] *Professor, Universidad Politécnica de Madrid, claudio.olalla@upm.es*

Abstract

Current simplified design methods for the seismic analysis of cut-and-cover underground structures are based on the quasi-static assessment of the structure shear distortion displacement, and then, evaluation of the internal forces through the analysis of a frame subjected to an imposed load pattern. However, two compelling and competing approaches are currently found in current building codes for addressing this issue.

On the one hand, American codes such as *NCHRP-611*, *FHWA Tunnel Design Manual 2009*, *AASHTO LRFD Road Tunnel Design Specifications 2017,* and some others inspired by these, advocate for the use of the so-called racking coefficient *R* when assessing the structure shear distortion: a single parameter trying to encompass the whole soil-structure interaction phenomena, which amplifies or reduces the free-field soil shear distortion. Once that the structure shear distortion is assessed, a triangular lateral pressure distribution is applied directly on the structure walls, such that the resulting distortion matches the one evaluated by multiplying the racking coefficient *R* times the free field distortion.

On the other hand, European, Japanese, Chilean, and other international codes such as *EN 1998-2:2004* and *Guide AFPS 2001*, *RTRI-2008, JSCE Cut-and-Cover Tunnel Specifications 2016*, *Manual de Carreteras 2016*, and *ISO-23469:2005(R2014),* respectively, advocate for a frame analysis jointly with a surrounding Winkler condition, and then application of the free-field soil shear distortion to the free ends of the Winkler springs, without any further amplification, assuming that the elastic foundation will cater for the soil-structure interaction phenomena.

However, both methods provide different results, which in turns are inaccurate in terms of structure internal forces as bending moment and shear when compared to numerical analyses and experimental measures, especially for the more flexible underground structures.

This paper addresses this unresolved issue, delves into the causes for these inaccuracies, and presents a summary for an improved, yet simple, methodology to compute internal forces of rectangular underground structures subjected to earthquake action. Moreover, it introduces a framework to reconcile the salient features of the aforementioned methods, in a format that could be considered for inclusion in building codes.

The results obtained by this proposed methodology are compared systematically to the results obtained by finite element analyses, by simplified methods proposed by other authors, and by the aforementioned building codes, for a wide range of structure geometries, flexibilities, and soil properties, and are proven to have an improved accuracy for prediction of internal forces respective to current simplified methods.

Keywords: racking; tunnel; Winkler; imposed-displacement; seismic

1. Introduction

Earthquake action on underground cut-and-cover structures is one more aspect that engineers shall consider when facing its design. In current international earthquake-resistant design codes, several distinct simplified techniques coexist to analyze the effects that seismic action bears on buried structures. Each of these methodologies may provide uneven results, in terms of internal forces like bending moments and shearing forces, especially when compared to more sophisticated analysis methods like finite element analyses (FEA). This lack of consistency in the analysis criteria across codes results into structures with different safety margins against earthquakes, depending on the particular analysis method selected, and especially for the more flexible structures presenting large underground spaces, like metro stations.

In particular, two distinct simplified methods outstand: On the one hand the method developed by Wang and Penzien [1, 2] (Wang method onwards) adopted by US codes [3-8] and others inspired by these, and on the other hand the method present in European [9-11], Japanese [12, 13], Chilean [14], and ISO [15] codes (E&J method onwards). Even though these two methods may look similar at a first glance, they present significant differences.

Both simplified methods assume that the seismic structure internal forces may be obtained by the analysis of a simple frame, representing the cut-and-cover structure, subjected to a differential displacement between the top and bottom slabs. Both simplified methods begin with the assessment of the maximum free-field soil shear deformation γ_{FF} during the earthquake, in the soil portion that will be substituted by the cut-and-cover structure. That is to say, given that a pure shear soil deformation pattern is assumed during the earthquake, the difference in lateral displacement between the buried structure top slab and the invert. Once that common step is taken, differences between both methods arise. In the following, we will address a critical description of these two methods.

On the one hand, the method proposed by Wang, and adopted in US codes, assumes that the structure lateral differential displacement is heavily influenced by soil-structure interaction, and that this effect may be encompassed by the so-called racking coefficient R. When obtaining the structure shear deformation γ_s, the racking coefficient R directly multiplies the free field shear strain γ_{FF}, as shown in Fig.1a.

Several authors [1-3, 16-17] have proposed different closed form-expressions for this racking coefficient R, or numerical values for a dense grid of cases [18]. Even though each study results in slightly different values, they share a common bottom line: the structural displacement depends on the relative shear distortion stiffness between the soil substituted by the structure and the structure itself, a parameter usually termed flexibility ratio F_R [1], and which is routinely assessed through a simple frame computer analysis. The more flexible structures deform more than the free-field, and conversely the stiffer structures deform less.

For deeply buried structures, Wang [1] proposes to apply a concentrated horizontal force at the top slab level such that the structure distortion γ_{STRU} matches the free-field shear distortion γ_{FF} amplified times the racking coefficient R value ($\gamma_{STRU}=R\cdot\gamma_{FF}$) (Fig. 1a), and for the shallower structures to apply a triangularly distributed wall pressure to match that same displacement value.

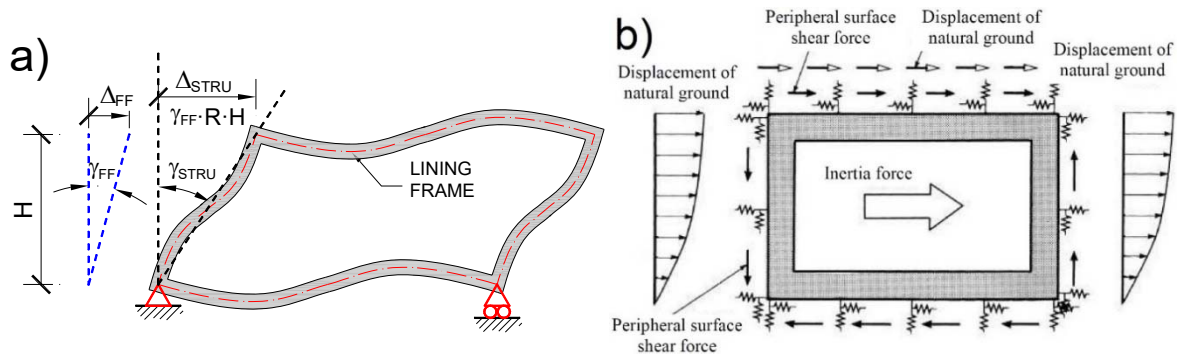

Fig. 1 – Sketch of current simplified methods. a) Wang method. b) European-Japanese (E&J) method [13].

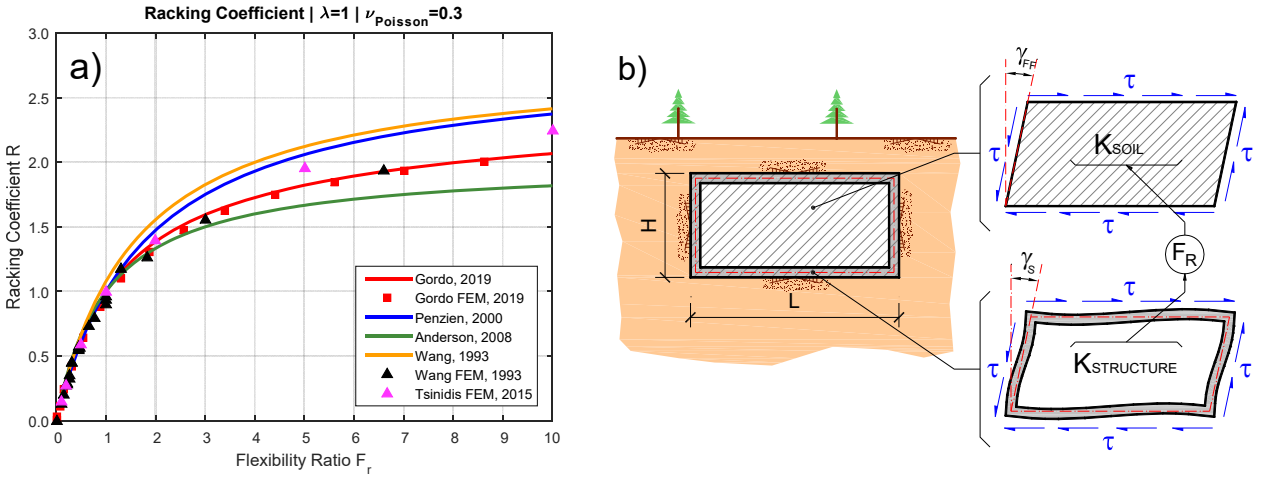

Fig. 2 – (a) Racking coefficient R for $\lambda=1$, $\nu=0.3$ as proposed by Wang [1], Penzien [2], Anderson et al. [3], Gordo-Monso et al. [17]. (b) Flexibility ratio F_R concept as defined by Wang [1].

However, several studies [19-23] have found that the internal forces predicted by the described procedure show significant differences to those obtained by means of finite element model analyses (FEM), and to those measured in laboratory tests [24-27] both in absolute value and in the shape of the internal force diagram. Moreover, for the case of extremely stiff structures like metro station end wall diaphragms, where $F_R \approx 0$ and $R \approx 0$, the resolution method is not well suited. For these cases, Wang [1] proposes to discard this technique and use the method proposed by Wood [28] to compute the pressure acting on walls. Nevertheless, the Wood method relies in the assumption that the stiff structure is founded on an infinitely stiff soil, which is not usually the case for cut and cover structures, and which contradicts the findings on rocking pattern behavior described by several authors [17-19, 22-24, 27, 29-30] for stiff underground structures.

On the other hand, the E&J method, in order to assess jointly the differential structural displacement and internal forces, proposes to directly apply the free-field displacement to a simple frame computer model complemented with Winkler top, bottom, and lateral boundaries (Fig. 1b). In the E&J method, the free-field displacement in-depth profile is applied to the free ends of the Winkler springs, as well as the free-field shear stresses arising at the soil portion that will be substituted by the buried structure. The E&J method does not consider any further soil displacement amplification (does not multiply the free-field deformation times the racking R coefficient), assuming that the Winkler foundation will cater for the soil-structure interaction effect.

This particular aspect of the E&J method (not considering the R factor) is an important issue which may yield inaccurate results in some cases. As an illustrative extreme example, albeit somewhat difficult to find in practice, we may consider the case of an infinitely flexible structure, namely a void space. Regarding the Wang method, the rectangular cavity shear deformation would correspond to a $R \approx 2.5$ free-field deformation, where the particular R value depends on the specific closed-form solution [1-3, 16-18], geometry, and soil Poisson coefficient. However, regarding the E&J method, given that the structure is infinitely flexible, the Winkler springs do not have anything to react against, and the structure-attached nodes would displace exactly the same amount as the nodes where the displacement is imposed, yielding a structure deformation identical to the free-field deformation.

In summary, for the case of very flexible structures the E&J method predicts structure displacements equal to the free-field, whereas the Wang method predicts displacements $\approx 250\%$ larger than the free-field ones. On the other end, for the case of extremely stiff structures, the E&J method is able to predict internal forces results, whereas the Wang method is not well suited for these cases and some other method should be used.

2. Purpose of the Proposed Simplified Improved Method

As exposed in the preceding section, several inaccuracies arise when using the described two trending analysis methods present in current seismic design codes for underground structures. Therefore, it would be desirable to have a single method which could be used confidently for the whole range of structural stiffness, able to deal with soil nonlinear behavior, and accurate when predicting structural deformations and internal forces. Ideally, this method would be intuitively easy to understand.

The method that we briefly outline here is aimed to fulfill the above expectations, and is based in the three following aspects: 1) Develop a closed-form expression for the racking coefficient R which would yield a deeper understanding of the mechanics involved in racking distortion. 2) Extend this expression for the case of nonlinear soil behavior. 3) Integrate the preceding aspects into a conceptual frame, to predict internal forces.

3. Closed Form for the Racking Coefficient, and Racking Profile

Consider a rectangular underground structure (of width b, depth d, and aspect ratio $\lambda=b/d$), and a portion of surrounding soil of arbitrary size (of width L and depth H) concentric with the underground structure as in Fig. 3a. Consider that the soil exterior perimeter is subjected to a pure shear stress state, and consider that our purpose is to determine the strain field in the soil and structure.

In determining the strain field, the following 3 assumptions are made:

- The soil-structure system can be divided in rectangular blocks, numbered 1 to 9 (Fig. 3a).
- Each block can only deform in a pure shear pattern (Fig. 3b), with the shear stiffness of an elastic, homogenous, and isotropic medium, defined by its shear modulus G and the elasticity equation $\gamma=\tau/G$. Note that this equation measures the total sheared angle γ between orthogonal boundaries, but that the sheared angle respective to the vertical and horizontal boundaries of the block is $\gamma/2$ each.
- There is displacement compatibility between corners of adjacent blocks, that is, corners shared by different blocks displace horizontally and vertically the same amount. This would translate to a non-slip condition in terms of previous studies [1-2].

Stemming from the above, it is assumed that within each block shear stresses and strains are constant through the entire width or depth, in particular at its boundaries. This means that no stress or strain concentration will take place in the corners of the soil-structure, and that only an "average stress" and "average strain" will be considered for each block. Moreover, the total angle γ sheared by each block will be the sum of the sheared angles γ_H and γ_V that produce horizontal and vertical displacements.

If one follows the transfer of, say, horizontal shear force from the top to the bottom boundary through the depth of the system, from equilibrium considerations, it is easy to note that the total shear force at any horizontal section must be constant (Fig. 4a) (even if the horizontal shear stress at each block may be different).

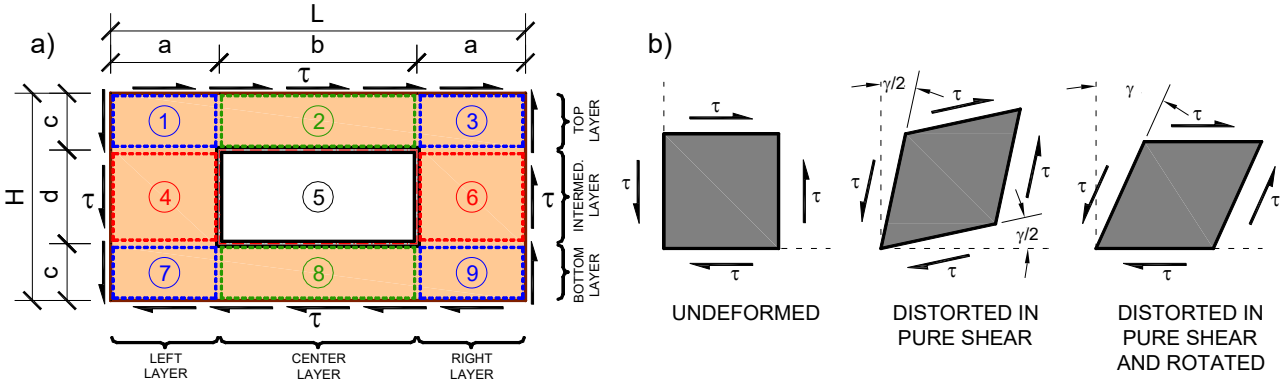

Fig. 3 – (a) Block diagram of a portion of the soil-structure system. (b) Pure shear strain scheme for a block.

Similarly, stemming from the above assumptions, and from displacement compatibility considerations between contiguous blocks, one can note that for each horizontally contiguous block (that is pertaining to the same horizontal layer, namely the top layer of blocks 1-3, the intermediate layer of blocks 4-6, and the bottom layer of blocks 7-9) the horizontal shear distortion strain γ_H must be of equal value.

Therefore, the horizontal displacement stiffness for each horizontal layer of blocks must be the in parallel sum of the shear stiffness of each of the three blocks within the layer. In particular, and considering that the horizontal displacement corresponds solely to the horizontal sheared angle $\gamma/2$, the stiffness $K_{n,H}$ of each block n for a horizontal force will be as shown in Eq. 1-5. Where the term F_R in Eq. 5 corresponds to the classical flexibility ratio as defined by Wang [1], which in the case of a linearly elastic single barrel rectangular tunnel of width b, depth d, and wall and slab bending inertias I_w and I_b respectively is defined by Eq. 6. A similar reasoning would be valid for the vertical shear force transferring right to left (Fig. 4b). Using appropriate dimensions, the stiffness $K_{n,V}$ of each block n for a vertical force will be as shown in Eq.1-5.

$$K_{1,H} = K_{3,H} = K_{7,H} = K_{9,H} = 2 \cdot G \cdot \frac{a}{c} \tag{1}$$

$$K_{1,V} = K_{3,V} = K_{7,V} = K_{9,V} = 2 \cdot G \cdot \frac{c}{a} \tag{2}$$

$$K_{2,H} = K_{8,H} = 2 \cdot G \cdot \frac{b}{c} \qquad K_{2,V} = K_{8,V} = 2 \cdot G \cdot \frac{c}{b} \tag{3}$$

$$K_{4,H} = K_{6,H} = 2 \cdot G \cdot \frac{a}{d} \qquad K_{4,V} = K_{6,V} = 2 \cdot G \cdot \frac{d}{a} \tag{4}$$

$$K_{5,H} = K_{STRU,H} = 2 \cdot \frac{G \cdot \frac{b}{d}}{F_R} \qquad K_{5,V} = K_{STRU,V} = 2 \cdot \frac{G \cdot \frac{d}{b}}{F_R} \tag{5}$$

$$F_R = \frac{K_{SOIL}}{K_{STRU}} = \frac{G \cdot \frac{b}{d}}{\frac{1}{\frac{d^2 \cdot b}{24 \cdot E \cdot I_b} + \frac{d^3}{24 \cdot E \cdot I_w}}} \tag{6}$$

From the previous expressions (Eq. 1-5), and owing to the shear strain compatibility between horizontal adjacent blocks, the shear stiffness for each horizontal layer (K_{TOP} for the top layer, K_{INT} for the intermediate, and K_{BOT} for the bottom layer) can be obtained as an in-parallel sum of stiffness (Eq. 7-8).

$$K_{TOP,H} = K_{BOT,H} = K_{1,H} + K_{2,H} + K_{3,H} = K_{7,H} + K_{8,H} + K_{9,H} = 2 \cdot G \cdot \frac{L}{c} \tag{7}$$

$$K_{INT,H} = K_{4,H} + K_{5,H} + K_{6,H} = 2 \cdot G \cdot \frac{2a}{d} + K_{STRU,H} \tag{8}$$

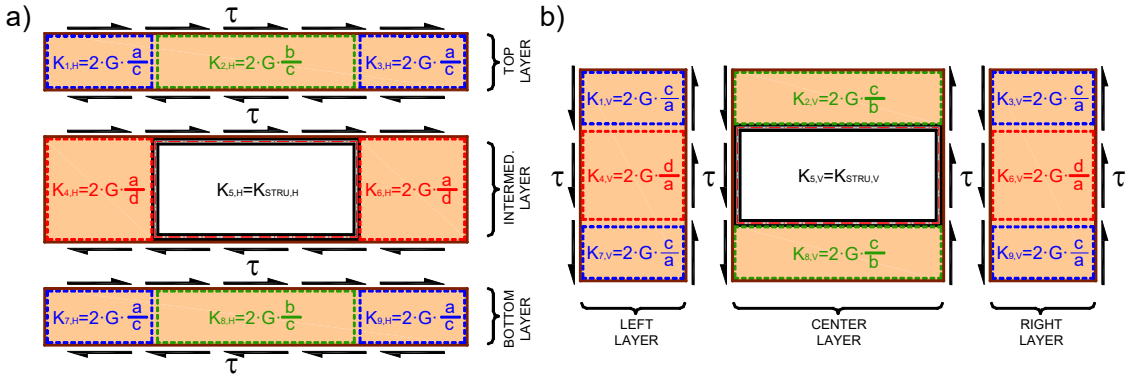

Fig. 4 – (a) Horizontal shear transfer. (b) Vertical shear transfer.

The shear stiffness for each vertical layer (K_{LEFT}, K_{CENT}, and K_{RIGHT} for the left, center, and right layers respectively) (Fig. 4b) can be obtained similarly as the in-parallel sum of corresponding stiffness (Eq. 9-10).

$$K_{LEFT,V} = K_{RIGHT,V} = K_{1,V} + K_{4,V} + K_{7,V} = K_{3,V} + K_{5,V} + K_{9,V} = 2 \cdot G \cdot \frac{H}{a} \tag{9}$$

$$K_{CENT,V} = K_{2,V} + K_{5,V} + K_{8,H} = 2 \cdot G \cdot \frac{2c}{b} + K_{STRU,V} \tag{10}$$

If one were to estimate the average horizontal shear stiffness $K_{AVG,H}$ of the soil and structure ensemble (that is the 9 blocks), by measuring the force required at the top face in order to produce a unit horizontal displacement, an appropriate method consistent with the above assumptions would be to sum the in-series stiffness of each horizontal layer (Eq. 11). Similarly for the average vertical shear stiffness $K_{AVG,V}$ of the soil and structure ensemble, adding the in-series stiffness of each vertical layer (Eq. 12).

$$K_{AVG,H} = \frac{1}{\frac{1}{K_{TOP,H}} + \frac{1}{K_{INT,H}} + \frac{1}{K_{BOT,H}}} = \frac{1}{2 \cdot \frac{1}{2 \cdot G \cdot \frac{L}{c}} + \frac{1}{2 \cdot G \cdot \frac{2a}{d} + K_{STRU,H}}} \tag{11}$$

$$K_{AVG,V} = \frac{1}{\frac{1}{K_{LEFT,V}} + \frac{1}{K_{CENT,V}} + \frac{1}{K_{RIGHT,V}}} = \frac{1}{2 \cdot \frac{1}{2 \cdot G \cdot \frac{H}{a}} + \frac{1}{2 \cdot G \cdot \frac{2c}{b} + K_{STRU,V}}} \tag{12}$$

With the previous results at hand, one can compute an approximate racking coefficient for the shear distortion of the embedded structure and the average shear distortion of the soil and structure ensemble, that is to say, the ratio of shear distortions between the inner structure $\gamma_{INN} = \gamma_{INT,H} + \gamma_{CENT,V}$ and the outer perimeter $\gamma_{AVG} = \gamma_{AVG,H} + \gamma_{AVG,V}$, when the outer perimeter is subjected to a pure shear stress state of value τ. This racking coefficient would be the ratio of the sum of strains as shown in Eq. 13.

$$\tilde{R} = \frac{\gamma_{INT,H} + \gamma_{CENT,V}}{\gamma_{AVG,H} + \gamma_{AVG,V}} = \frac{\frac{\tau \cdot L / K_{INT,H}}{d} + \frac{\tau \cdot H / K_{CENT,V}}{b}}{\frac{\tau \cdot L / K_{AVG,H}}{H} + \frac{\tau \cdot H / K_{AVG,V}}{L}} = \frac{\frac{L}{d \cdot K_{INT,H}} + \frac{H}{b \cdot K_{CENT,V}}}{\frac{L}{H \cdot K_{AVG,H}} + \frac{H}{L \cdot K_{AVG,V}}} \tag{13}$$

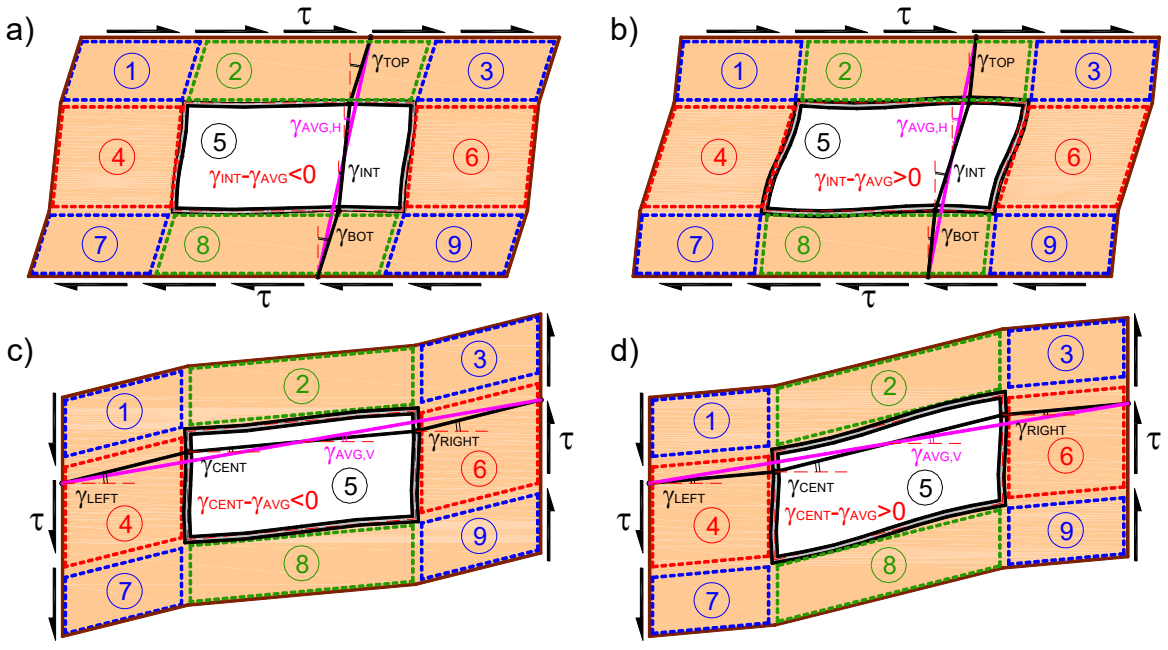

Fig. 5 – Horizontal shear deformation for a structure: (a) Stiffer than soil ($F_R<1$). (b) Softer than soil ($F_R>1$). Vertical shear deformation for a structure: (c) Stiffer than soil ($F_R<1$). (d) Softer than soil ($F_R>1$).

From the previous expressions, and for the sake of simplicity considering only the horizontal shear strain contribution, one can readily obtain some important information. As it would be expected, if the intermediate layer were stiffer than the soil-structure ensemble, the intermediate layer would deform less than the ensemble (Fig. 5a). On the contrary, if the intermediate layer were softer, the intermediate layer would deform more than the soil and structure ensemble (Fig. 5b). Notice that the distortion stiffness of the intermediate layer is governed by the distortion stiffness of the embedded structure: a small structure stiffness when compared with the substituted soil ($F_R>1$) would yield an intermediate layer softer than the ensemble, and vice versa. A similar reasoning can be made regarding the vertical component of the shear strain, as depicted in (Fig. 5c-d).

Until this point in the discussion, the dimensions L and H for the soil perimeter have been chosen arbitrarily. If we think for which dimensions the block assumptions may be approximately valid, we may consider that, for a soil perimeter close enough to the structure, the average shear distortion can be assumed constant in each layer. Therefore, we may think that we can compute approximately a racking coefficient between a soil perimeter close enough to the structure and the structure itself by means of Eq. 13.

Moreover, we may assume that if we consider successive soil control perimeters (Fig. 6a), close enough one to each other (say perimeters i-1 and i), we may compute an approximate individual racking coefficient $\tilde{R}_i$, relating the shear distortion of these, using Eq.13. For doing so in any control perimeter i, it will suffice to substitute the structure stiffness $K_{STRU,H}$ and $K_{STRU,V}$ in Eq. 11-12 with the average horizontal and vertical stiffness of the more internal perimeter i-1, $K_{AVG,H,i-1}$ and $K_{AVG,V,i-1}$, and to choose geometrical dimensions a_i, b_i, c_i, d_i, L_i and H_i corresponding to the given control perimeter i, as in Eq. 14.

$$\tilde{R}_i = \frac{\gamma_{AVG,H,i-1}+\gamma_{AVG,V,i-1}}{\gamma_{AVG,H,i}+\gamma_{AVG,V,i}} = \frac{\frac{L_i}{d_i \cdot K_{INT,H,i-1}}+\frac{H_i}{b_i \cdot K_{CENT,V,i-1}}}{\frac{L_i}{H_i \cdot K_{AVG,H,i}}+\frac{H_i}{L_i \cdot K_{AVG,V,i}}} \tag{14}$$

If we follow the reasoning, we may think that the total racking coefficient relating the embedded structure shear distortion γ_{STRU}, and the free-field distortion γ_{FF}, can be approximated by a sufficiently large portion of soil surrounding the structure with a fine discretization of successive control perimeters, and by the product of each individual racking coefficient as in the multiplicative Eq. 15 (Fig. 6a).

$$R = \frac{\gamma_{STRU}}{\gamma_{FF}} \cong \prod_{i=1}^{i=n} \frac{\gamma_{i-1}}{\gamma_i} = \prod_{i=1}^{i=n} \tilde{R}_i \tag{15}$$

In Eq. 15 the $\tilde{R}_i$ expression is given by Eq. 14, and in Eq. 14 for $i=1$ corresponding to the innermost control perimeter, the $K_{AVG,H,i-1=0}$ and $K_{AVG,V,i-1=0}$ are the structure stiffness given by Eq. 5.

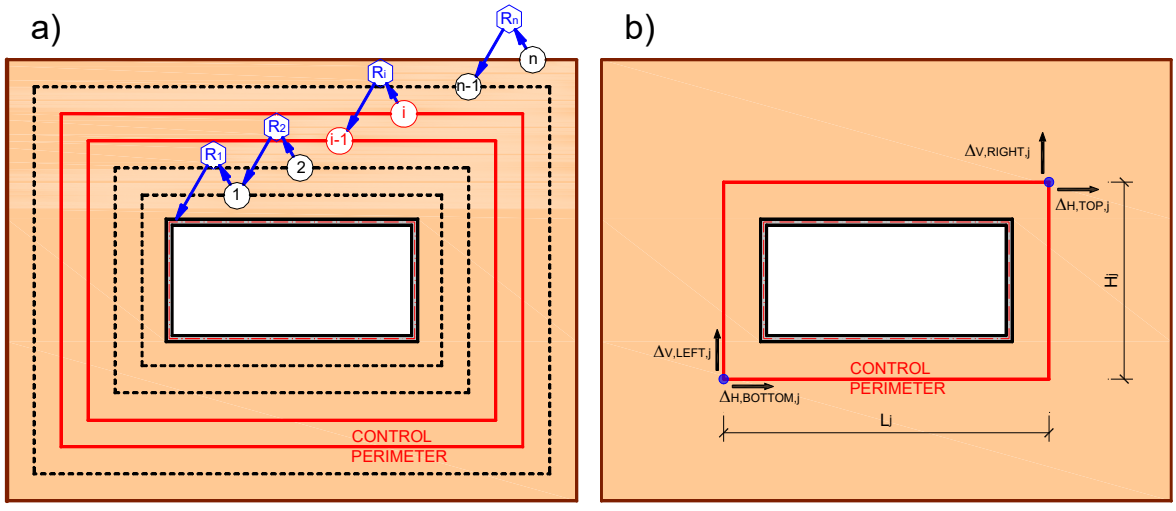

Fig. 6 – (a) Successive series of control perimeters 1 to n. and individual racking coefficients $\tilde{R}_i$. (b) Displacement control points for a control perimeter j to compute intermediate racking coefficients with FEM.

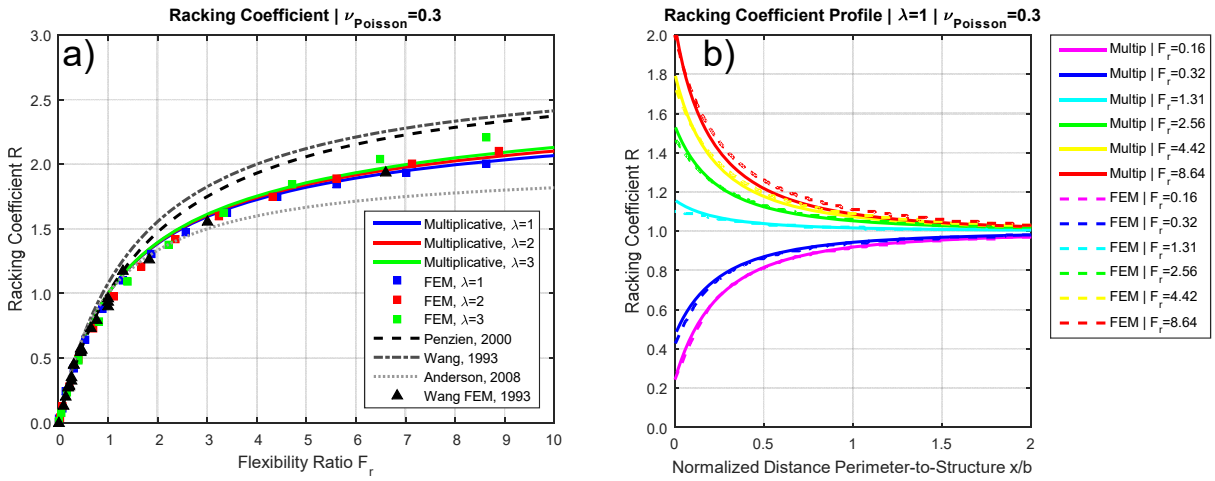

Fig. 7 – (a) Racking coefficient R as per the proposed closed-form, FEM analysis, and other authors [1-3]. (b) Racking coefficient profile as per the proposed closed-form and FEM analyses.

In order to verify the accuracy of the proposed closed-form solution for the racking coefficient, a series of finite element models (FEM) have been carried out in OpenSEES [31]. The FEM analyses developed represent the problem of a sufficiently large elastic, isotropic, and homogenous soil medium with an embedded rectangular structure at its center. The soil external boundaries are subjected to a pure shear stress state of value τ. The considered soil shear wave velocity is V_S=*360* m/s and the soil specific weight of ρ= *20* kN/m^3, yielding a shear modulus G = *259.20* MPa. Regarding the tunnel, a concrete structure has been considered with Young modulus E_c = *30* GPa, and constant wall and slab thickness of $h_w = h_b$ = *1.50* m providing the gross bending inertia. The width b and depth d dimensions of the structure have been varied from *1* m to *20* m. Different structure aspect ratios λ=b/d ranging from 1 to 3 have been analyzed to study its influence on the solution. The soil boundaries, both for the FEM analyses and the closed form solutions proposed in this paper have been chosen *50* m away horizontally and vertically from the structure. The chosen discretization for the closed form has been *1000* perimeters. Fig. 7a shows a very good agreement of the proposed multiplicative solution Eq. 15 with the FEM analyses for all the studied aspect ratios.

We might also consider to analyze and compare the profile of the racking coefficient at different distances (close and far from the structure), that is, how much an intermediate perimeter distorts respective to the free-field distortion γ_{FF}. Regarding the multiplicative closed-form method presented in the previous section, an expression similar to Eq. 15 to compute such profile for a given perimeter j would be Eq. 16.

$$R_{PERIM\ j} = \frac{\gamma_{PERIM\ j}}{\gamma_{FF}} \cong \prod_{i=j+1}^{i=n} \frac{\gamma_{i-1}}{\gamma_i} = \prod_{i=j+1}^{i=n} \tilde{R}_i \tag{16}$$

As for the racking coefficient, the same set of FEM analyses has been used to obtain numerical results for the racking profile. The average shear distortion $\gamma_{FEM,PERIM\ j}$ at each control perimeter j in the FEM analyses has been computed as the horizontal and vertical displacement difference for the bottom leftmost corner and the top rightmost corner of each perimeter with Eq. 17 (Fig. 6b), and then normalized by the free-field distortion γ_{FF} to obtain the racking profile at each perimeter j.

$$\gamma_{FEM,PERIM\ j} = \frac{\Delta_{HORIZ,TOP,j} - \Delta_{HORIZ,BOTTOM,j}}{H_j} + \frac{\Delta_{VERT,RIGHT,j} - \Delta_{VERT,LEFT,j}}{L_j} \tag{17}$$

Results are shown in (Fig. 7b) where the horizontal abscissa has been normalized among models as the ratio of the distance of the control perimeter to the structure X, divided by the structure width b ($X_{PERIMETER}/b_{STRUCTURE}$=*0* means a perimeter adjacent to the structure, and $X_{PERIMETER}/b_{STRUCTURE}$=*2* two widths from the structure). In Fig. 7b the multiplicative expression Eq. 16 shows a very good agreement with the FEM, and indicates that a distance of *1.5* to *2* structure widths the influence of the embedded structure becomes almost negligible.

4. Consideration of Nonlinear Soil Behavior

Large ground motions are expected to develop large soil strains, and hence, nonlinear behavior. A rational method to incorporate nonlinear soil behavior would be to perform the computation of the racking coefficient R by means of Eq. 15, but with a reduced soil stiffness which would consider the strain level reached at every point in the surrounding soil. Regarding the proposed method, this can be easily done by modifying the constant value G in Eq.1.-5, to the secant-reduced value corresponding to each control perimeter G_j. Given that the whole racking coefficient profile $R_{PERIM\,j}$ (Fig. 7b) is known, the racking deformation for each perimeter can be computed as $\gamma_{PERIM\,j} = \gamma_{FF} \cdot R_{PERIM\,j}$, and G_j by means of the corresponding stiffness reduction curve.

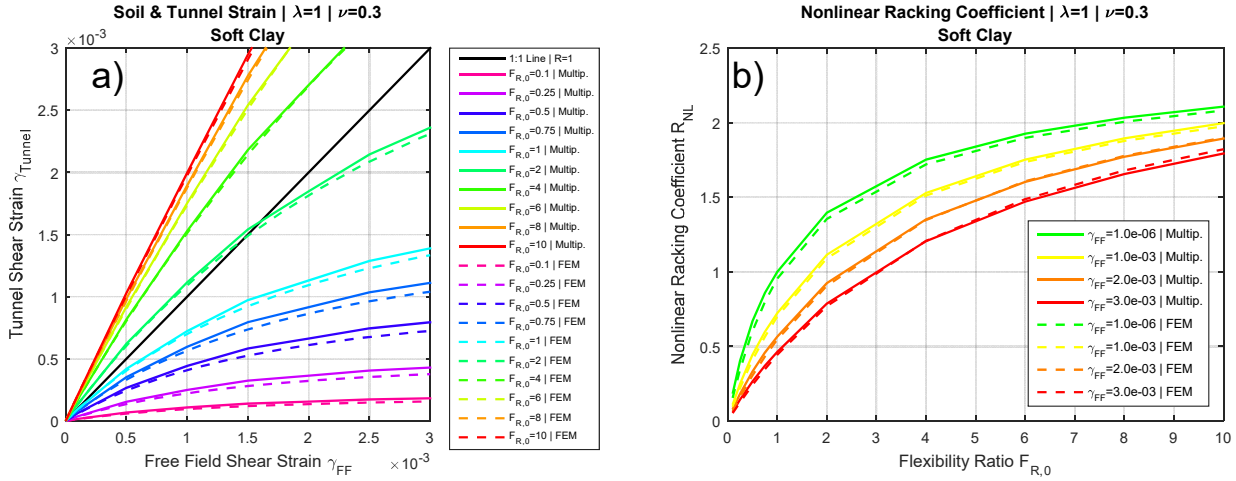

Fig. 8 – (a) Structure deformation as a function of free-field deformation. (b) Nonlinear racking coefficient.

To assess the accuracy of the proposed technique, a series of FEM analysis have been carried out in OpenSEES, with soil non-linear behavior as provided by the *PressureIndependMultiYield* material [32] for soft, medium, and stiff clays. Results obtained by the proposed simplified method and FEM analyses present a very good agreement. Fig. 9a shows the embedded structure shear strain γ_{Tunnel} as a function of the soil free-field shear strain γ_{FF}, while Fig. 9b shows traditional racking coefficient curves for different free-field shear strains γ_{FF}, and both show how soil stiffness reduction decreases the racking coefficient for large soil strains.

5. Improved Method for the Analysis of Bending Moments and Shear Forces

Once that the structure racking deformation is obtained, whether for the soil linear or nonlinear behavior, appropriate assessment of the structure internal forces must be done. Some current simplified methods, such as the one proposed by Wang [1] (Fig. 9a) are able to approximately predict the shearing deformation of underground structures, but provide inaccurate results in terms of internal forces. Therefore, the question arises of what are the mechanical effects that come into play precluding to predict accurately bending moments and shear forces, but which do not influence the overall deformational behavior of the structure.

The mechanism proposed in this study to explain this behavior is that of the local surrounding soil reaction. As the structure distorts in shear, the members local bending (i.e. slabs and walls) produces outwards and inwards deflections out of the geometrical planes defined by the corners of the structure. These deflections induce a set of local mutual reactions between the surrounding soil and the structure lining, which in turns modify the deflection of the members and therefore the internal forces.

To predict such a local behavior, and to improve the assessment of the lining internal forces, a simple model is proposed as in Fig 9b. Conceptually, we may think that, once that the overall structure distortion is imposed to the underground frame, the local mutual reaction of the soil and structure can be modelled through a series of Winkler springs. Given that the structure and surrounding soil are already distorted by an imposed displacement, the Winkler foundation should not link the structure members to an outer undefined boundary,

but to a frame of reference which is able to move along with the lining in its racking distortion. This frame of reference represents the average line of contact between soil and structure, and can be represented appropriately in a simple frame computer model by a set of infinitely stiff beams (i.e. much stiffer than the lining members stiffness), which are linked to the lining frame corner nodes, and provided with flexural hinges at these corners. This stiff-beams reference frame is then linked to the adjacent lining frame by a set of Winkler springs which represent the local soil-structure interaction. For the value of the Winkler spring stiffness, the expression proposed by Vesic [33] has been found to provide results accurate enough. However, this does not preclude the use of other values for the Winkler stiffness as determined from field tests, which could be more representative of the conditions for the particular case at hand.

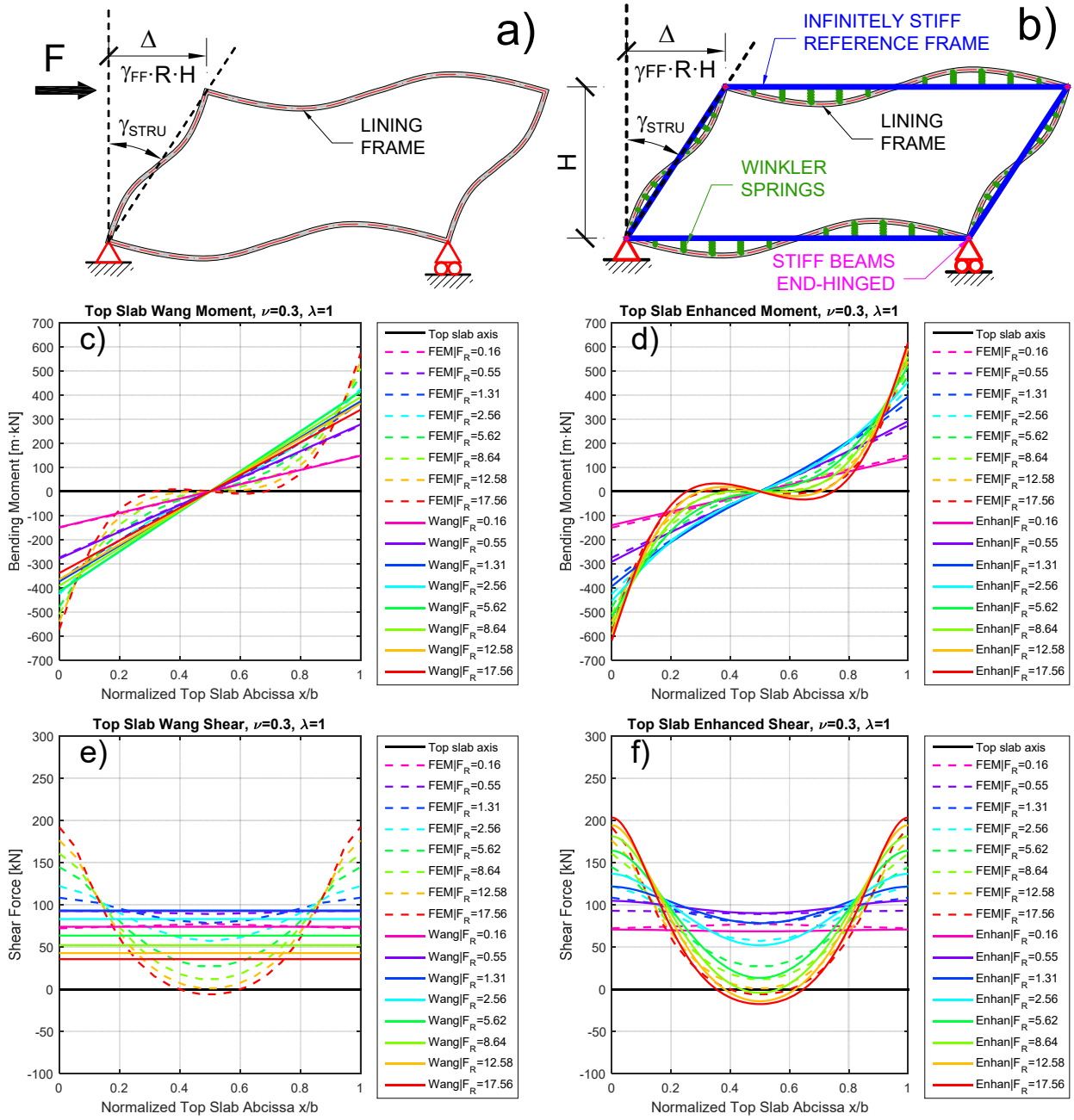

Fig. 9 – Sketch of (a) Wang method. (b) Proposed method. Top slab bending moments diagram as per: (c) Wang method. (d) Proposed method. Top slab shear as per: (e) Wang method. (f) Proposed method.

Fig. 9 shows the comparison of internal forces obtained by the Wang [1] method, proposed improved method, and FEM analyses. Fig. 9c and Fig. 9e compare bending moments and shear in the structure top slab as per Wang method and the FEM analyses. Fig. 9d and Fig. 9f do the same for the proposed improved method.

As it is readily apparent, the Wang method provides accurate results for the stiffer structures, but present large differences for the softer structure cases. In particular, it fails both to predict the shape of the bending moment and shear diagrams. Wang method predicts the slab to behave as a beam in double bending with constant shear, while the FEM analyses predict more convoluted shapes, with sharp increases in moments and shear towards the end sections for the softer structure cases. On the other hand, the results obtained with the proposed simplified method show a very good agreement to the FEM results. In particular, the proposed improved method is able to capture the sharp increase both in moment and shear at the end of the slab.

6. Conclusion

A simple improved method to accurately predict bending moments and shear forces in rectangular underground structures subjected to earthquake action has been succinctly presented. The results provided by this method have been compared to those obtained with finite element analyses, and it is shown to be more accurate than current simplified approaches. The proposed method can be thought to be a blend of the two major trends present in international earthquake resistant design codes addressing the analysis of underground structures.

The method consists of three steps: 1) assessment of the soil-structure racking deformation, 2) reevaluation of the racking deformation in order to consider soil non-linear behavior, 3) assessment of the structure internal forces with a simple frame model, with Winkler springs, and with a stiff reference frame.

The method can be very easily implemented with a spreadsheet and a simple frame computer model, similar to those currently used in the racking-stiffness assessment of underground structures with limited extra effort, but more importantly, it provides a simple conceptual framework to understand the mechanic behavior of a rectangular structure embedded in a surrounding medium, subjected to the earthquake action.

7. References

[1] Wang, J. N. (1993): *Seismic Design of Tunnels. A Simple State of the Art Approach*. Parsons-Brinckerhoff, New York, USA, 1-159.

[2] Penzien, J. (2000): Seismically induced racking of tunnel linings. *Earthquake Engineering & Structural Dynamics*, **29** (5), 683-691.

[3] Anderson, D. G. Martin, G. R. Lam, I. Wang, J. N. (2008): Seismic Analysis and design of Retaining Walls, Buried Structures, Slopes, and Embankments. *NCHRP Report 611*. TRB, Washington-DC, USA.

[4] Hung, C. J. Monsees, J. E. Munfah, N. Wisniewski, J. (2009): *Technical Manual for Design and Construction of Road Tunnels – Civil Elements*. FHWA-NHI-10-034. US Dept. of Transportation. Federal Highway Administration. Washington-DC, USA.

[5] AASHTO, American Association of State Highway Officials. (2017): LRFD Road Tunnel Design and Construction Guide Specifications. Washington-DC, USA.

[6] Los Angeles County Metropolitan Transportation Authority. (2012): *Metro Rail Design Criteria. Section 5 Structural. Appendix Metro Supplemental Seismic design Criteria*, Los Angeles, USA.

[7] Waggoner, F. Jacob, V. Jong, K. Van Winkle, H. (2011): Seismic Design Criteria, Structures Supporting High-Speed Trains. *California High-Speed Train Project. Technical Memorandum TM 2.10.4*. Sacramento, USA.

[8] WSDOT, Washington State Department of Transportation. (2010): *Appendix B8: SR 99 Tunnel Design-Build Project Seismic Design Criteria*. Alaskan Way Viaduct and Seawall Replacement Program. Seattle, USA.

[9] CEN, Comité Européen de Normalisation. (2005): *EN 1998-2. Eurocode 8 – Design of structures for earthquake resistance. Part 2: Bridges*. Brussels, Belgium.

[10] CEN, Comité Européen de Normalisation. (2004): *EN 1998-5. Eurocode 8 – Design of structures for earthquake resistance. Part 5: Foundations, retaining structures and geotechnical aspects*. Brussels, Belgium.

[11] AFPS, (2001): *Conception et protection parasismiques des ouvrages souterrains*, Paris, France.

[12] RTRI, Railway Technical Research Institute. (2007): Design standards for Railway Structures and Commentary (Seismic Design). Ministry of Land, Infrastructure and Transport. Tokyo, Japan.

[13] JSCE, Japan Society of Civil Engineers. (2018): *Standard Specifications for Tunneling-2016: Cut-and-Cover Tunnels*. Tokyo, Japan.

[14] Dirección de Vialidad. Ministerio de Obras Públicas. (2016): *Manual de Carreteras. Vol. 3. Instrucciones y Criterios de diseño*. Santiago, Chile.

[15] ISO, International Organization for Standardization. (2005): *ISO 23469:2005(E). Bases for design of structures – Seismic actions for designing geotechnical works*. 2014 Revision. Geneva, Switzerland.

[16] Huo, H. Bobet, A. Fernandez, G. Ramirez. J. (2006): Analytical solution for deep rectangular structures subjected to far-field shear stresses. *Tunn Undergr Sp Tech*, **21** (6), 613-625.

[17] Gordo-Monso, C. Gonzalez-Galindo, J. Olalla-Marañon, C. (2019): A closed-form solution for the seismic racking and rocking behavior of rectangular tunnels. *Tunn. and Undg. Sp Tech*, **88** (2), 89-97.

[18] Tsinidis, G., Pitilakis, K. (2018): Improved R-F relations for the transversal seismic analysis of rectangular tunnels. Soil Dynamics and Earthquake Engineering. **107**, 48–65.

[19] Debiasi, E., Gajo, A., Zonta, D. (2013): On the seismic response of shallow-buried rectangular structures. *Tunn Undergr Sp Tech*, **38**, 99–113.

[20] Tsinidis, G., Pitilakis, K., Anagnostopoulos, C., Madabhushi, G. (2015): Seismic response and Design of Rectangular Tunnels, *SECED 2015 Conference*, Cambridge, UK.

[21] Pitilakis, K., Tsinidis, G. (2014): Performance and Seismic Design of Underground Structures, in: Maugeri, M., Soccodato, C. (Eds.), *Geotechnical, Geological and Earthquake Engineering*. 279–340.

[22] Pitilakis, K., Tsinidis, G. (2016): Recent advances on the seismic behaviour and design of tunnels, *Conference in Honour of Michele Maugeri*, Catania, Italy.

[23] Tsinidis, G. (2017): Response characteristics of rectangular tunnels in soft soil subjected to transversal ground shaking. *Tunn Undg Sp Tech*, **62**, 1–22.

[24] Tsinidis, G., Pitilakis, K., Heron, C. (2015): Dynamic response of flexible square tunnels : centrifuge testing and validation of existing design methodologies. *Geotechnique*, **65**, 401–417.

[25] Abuhajar, O., Naggar, H., Newson, T. (2015): Seismic soil–culvert interaction. *Can. Geotech .J.*, **52**, 1649–1667.

[26] Cilingir, U., Madabhushi, S.P.G. (2012): Effect of depth on the seismic response of square tunnels. *Soils and Foundations*, **51**, 449–457.

[27] Cilingir, U., Madabhushi, S.P.G. (2011): A model study on the effects of input motion on the seismic behaviour of tunnels. *Soil Dynamics and Earthquake Engineering*, **31**, 452–462.

[28] Wood, J. (1973): *Earthquake Induced Soil Pressures on Structures*. Ph.D. Thesis. Caltech. Pasadena, USA.

[29] Iwatate, T., Kobayashi, Y., Kusu, H., Rin, K. (2000): Investigation and Shaking Table Tests of Subway Structures of the Hyogoken-Nanbu Earthquake, *12th WCEE*. Auckland, New Zealand.

[30] Ulgen, D., Saglam, S., Ozkan, M.Y. (2015): Dynamic response of a flexible rectangular underground structure in sand: centrifuge modeling. *Bulletin of Earthquake. Engineering*. 13, 2547–2566.

[31] McKenna, F., Scott, M.H., Fenves, G.L. (2010): Nonlinear Finite-Element Analysis Software Architecture Using Object Composition. *J. Comput. Civ. Eng*. **24**, 95–107.

[32] Gu, Q. Conte, J. Yang, Z. Elgamal, A. (2011): Consistent tangent moduli for multi-yield-surface J2 plasticity model. *Computational Mechanics*. **48**, (1), 97-120.

[33] Vesic, A. (1963): Beams on Elastic Subgrade and the Winkler's Hypothesis. *Proceedings of 5th International Conference of Soil Mechanics*, 845-850.

